

- (16) Venanzi, L. M. *J. Chem. Soc.* **1958**, 719.  
 (17) Nakamoto, K. "Infrared Spectra of Inorganic and Coordination Compounds", 2nd ed.; Wiley: New York, 1970; pp 160-166.  
 (18) Samuel, D.; Wasserman, I. *J. Labelled Compd.* **1971**, 7, 355.  
 (19) Shakhshiri, B. Z.; Gordon, G. *Talanta* **1966**, 13, 142.  
 (20) Although a substantial molar excess of CO is passed through the solution during the time necessary for complete reaction, the amount of CO which remains *in solution* is considerably less. The concentration of CO in a saturated solution at 11 °C can be estimated as  $6.6 \times 10^{-3}$  M from the reported solubility,<sup>21</sup> the known vapor pressure of benzene,<sup>22</sup> and assuming Henry's law is obeyed. For comparison, the initial concentration of nickel complex is  $6.7 \times 10^{-2}$  M.  
 (21) Linke, W. F. "Solubilities of Inorganic and Metal-Organic Compounds", Vol. 1; 4th ed.; American Chemical Society: Washington D.C., 1958; p 456.  
 (22) Timmermans, J. "Physico-Chemical Constants of Pure Organic Compounds", Vol. 2; Elsevier: Amsterdam, 1965; p 94.  
 (23) Muller, N.; Lauterbur, P. C.; Goldenson, J. *J. Am. Chem. Soc.* **1956**, 78, 3557.  
 (24) Feltham, R. D. *Inorg. Chem.* **1964**, 3, 116.  
 (25) Rossi, M.; Sacco, A. *Chem. Commun.* **1971**, 694.  
 (26) Tolman, C. A. *Chem. Soc. Rev.* **1972**, 1, 337.  
 (27) Enemark, J. H. *Inorg. Chem.* **1971**, 10, 1952.  
 (28) Tolman, C. A. *Chem. Rev.* **1977**, 77, 313.  
 (29) Ugo, R.; Bhaduri, S.; Johnson, B. F. G.; Khair, A.; Pickard, A.; Benn-Taarit, Y. *J. Chem. Soc., Chem. Commun.* **1976**, 694.  
 (30) Clearly, a quantitative comparison of the relative rates of oxygen-atom scrambling and CO<sub>2</sub> dissociation is dependent upon the mechanism invoked. We feel that such a comparison is unwarranted until such a time that detailed kinetic data are available.  
 (31) Aresta, M.; Nobile, C. F.; Albano, V. G.; Forni, E.; Manassero, M. *J. Chem. Soc., Chem. Commun.* **1975**, 636; Aresta, M.; Nobile, C. F. *J. Chem. Soc., Dalton Trans.* **1977**, 708.  
 (32) Herskovitz, T.; Guggenberger, L. J. *J. Am. Chem. Soc.* **1976**, 98, 1615.

## Porphyrin Core Expansion and Doming in Heme Proteins. New Evidence from Resonance Raman Spectra of Six-Coordinate High-Spin Iron(III) Hemes

Thomas G. Spiro,\* John D. Stong, and Paul Stein

Contribution from the Department of Chemistry, Princeton University, Princeton, New Jersey 08540. Received July 3, 1978

**Abstract:** Resonance Raman spectra are reported for high-spin bis(dimethyl sulfoxide) (Me<sub>2</sub>SO)<sub>2</sub>Fe<sup>III</sup> complexes of protoporphyrin IX dimethyl ester (PP), octaethylporphyrin (OEP), and tetraphenylporphyrin (TPP), and for aquo- and fluoromethemoglobin (Hb) and myoglobin (Mb), with emphasis on the three bands (II, IV, and V) which have previously been shown to be sensitive to iron spin state. These frequencies are essentially the same for [(Me<sub>2</sub>SO)<sub>2</sub>Fe<sup>III</sup>PP]<sup>+</sup> as for aquo-metHb and Mb, which had previously been thought to be anomalously low. Since recent crystal structure determinations have shown the high-spin bis-aquo and bis(tetramethylene sulfoxide) complexes of Fe<sup>III</sup>TPP to be planar porphyrins, with expanded cores, this experiment strongly supports core expansion as the determinant of the metHb and Mb spin-marker frequencies, and renders the hypothesis of protein-induced doming unlikely. Since protein crystallography has placed the iron atom 0.40 Å from the mean heme plane in metMb and 0.23 and 0.07 Å from the mean heme plane in the β and α chains of metHb, the lack of any associated variation in the spin-marker frequencies indicates that the core size is not determined by the disposition of the iron atom, but probably by steric interactions of the axial ligands with the porphyrin nitrogen atoms. Binding of fluoride to metHb and Mb leaves bands II and V unshifted, but lowers band IV by 5 cm<sup>-1</sup>. The similarity in spin-marker frequencies between native horseradish peroxidase (HRP) or cytochrome c' and the previously studied five-coordinate Fe<sup>III</sup> hemes indicates that these proteins contain five- rather than six-coordinate Fe<sup>III</sup> hemes; in the case of HRP six coordination is accessible with exogenous ligands. It is suggested that the intermediate-spin state observed for these proteins results from weakening of the bond between Fe<sup>III</sup> and the single axial ligand. The correlation with core size of the spin-marker frequencies is reexamined. Nonplanar hemes are found to have frequencies that are significantly depressed, presumably due to loss of π conjugation at the methine bridge. The relation between pyrrole tilt and the methine dihedral angles is derived for both ruffled and domed hemes, and is used to develop a simple relation that satisfactorily reproduces the spin-marker frequencies for both planar and nonplanar hemes. This model gives reasonable estimates of the σ and π contributions to the methine bond-stretching force constant. It is concluded that both core expansion and pyrrole tilting contribute to frequency lowerings, with core expansion dominant for moderate tilt angles. There is no evidence in any of the heme proteins so far studied of extra doming induced by the protein.

### Introduction

Resonance Raman spectra of heme proteins contain a rich assortment of porphyrin vibrational modes, whose frequencies have been well catalogued.<sup>1-7</sup> Some of the modes are sensitive to chemical alterations at the central iron atom, and are therefore of great interest as potential structure monitors. In an early study<sup>2</sup> it was observed that one set of bands was sensitive to changes in oxidation state of the iron atom while another set was sensitive to changes in its spin state. The oxidation state marker bands were suggested<sup>2,7a</sup> to be responding to changes in porphyrin π\* orbital occupancy via back-donation from the iron d<sub>π</sub> orbitals. This interpretation was subsequently confirmed<sup>8</sup> with a graded series of π-acceptor axial ligands, which compete with the porphyrin ring for the iron d<sub>π</sub> electrons. An interesting consequence of this mechanism is that π-donor ligands can shift the oxidation state marker

frequencies to values below the typical ones associated with nonacceptor ligands, as has recently been observed by Champion and Gunsalus<sup>6</sup> and by Kitagawa et al.<sup>7b</sup> for cytochrome P<sub>450</sub>, which is believed to have cysteine mercaptide, a π donor, as an axial ligand.

With respect to the spin-state marker bands our interpretation<sup>2</sup> was that the frequency decreases observed for high-spin hemes resulted from a doming of the porphyrin ring accompanying the well-known out-of-plane displacement of the iron atom toward the proximal ligand.<sup>9</sup> The pyrrole rings are expected to tilt, in order to maintain overlap with the iron orbitals, but this would be at the expense of π conjugation at the porphyrin methine bridges, resulting in the observed frequency lowerings. A subsequent normal-coordinate calculation<sup>10a</sup> indicated that this mechanism could account for the experimental data. A discrepancy between the spin marker

frequencies of aquomethemoglobin (metHb) and of five-coordinate high-spin  $\text{Fe}^{\text{III}}$  heme suggested an enhanced degree of doming for this form of the protein.<sup>8</sup>

A different interpretation of the spin marker band (band IV) at  $\sim 1580\text{ cm}^{-1}$ , which is easily recognized via its anomalous polarization,<sup>10b</sup> was advanced by Spaulding et al.,<sup>11</sup> who observed large decreases in this frequency for planar porphyrins with large atoms at their center, such as  $\text{Sn}^{\text{IV}}$  and  $\text{Ag}^{\text{I}}$ . To accommodate these atoms the porphyrin core is forced to expand, and Spaulding et al. found an inverse correlation between the band IV frequency and  $\text{C}_1\text{-N}$ , the distance from the center of the porphyrin to the pyrrole nitrogen atoms. The effect derives from stretching and bending of the methine bridge bonds which is observed to correlate with  $\text{C}_1\text{-N}$ .<sup>9,11</sup> Warshel's potential energy calculations<sup>12</sup> confirm that porphyrin core expansion is accommodated by methine bridge bond stretching and deformation.

Spaulding et al.<sup>11</sup> suggested that core expansion was also responsible for the band IV frequency shifts in heme proteins, and that the out-of-plane displacement of the iron atom could be calculated by triangulation, on the assumption of fixed radii for high- and low-spin iron(II) and -(III). They concluded that the anomaly between metHb and five-coordinate  $\text{Fe}^{\text{III}}$  porphyrin required an extra expansion of the porphyrin core in the protein, possibly induced by coordination of the sixth ligand,  $\text{H}_2\text{O}$ , which might pull the iron atom closer to the heme plane. At the time we believed this inference to be implausible, since we expected<sup>8</sup> that movement of the iron atom into the porphyrin ring would be accommodated by emptying of the in-plane  $d_{x^2-y^2}$  orbital, via spin pairing, and a resultant contraction, rather than expansion of the porphyrin core. This effect had been established for iron(II) tetraphenylporphine (TPP), which, in the absence of any axial ligand, adopts a structure with the iron atom in the center of a contracted porphyrin core; the depopulation of  $d_{x^2-y^2}$  is reflected in an intermediate spin state.<sup>13</sup>

Subsequent events, however, have shown this reasoning to be inapplicable to high-spin  $\text{Fe}^{\text{III}}$  with two axial ligands. Refinement of the metHb crystal structure<sup>14</sup> has revised downward the estimate of the out-of-plane iron displacement to 0.23 and 0.07 Å for the  $\beta$  and  $\alpha$  chains. And recently the bis(dimethyl sulfoxide) adduct of  $\text{Fe}^{\text{III}}$ TPP has been shown by NMR to be high spin in solution,<sup>15</sup> while the crystal structure of the high-spin bis-aquo<sup>16</sup> and bis(tetramethylene sulfoxide)<sup>17</sup> complexes of  $\text{Fe}^{\text{III}}$ TPP reveal an in-plane iron atom with an expanded porphyrin core. These crystallographic findings provide an important test of the core expansion hypothesis, which requires that planar six-coordinate high-spin  $\text{Fe}^{\text{III}}$  hemes show spin marker frequencies appreciably lower than out-of-plane five-coordinate derivatives. The results of the present study confirm this prediction. They establish that six coordination is a sufficient explanation of the low spin-marker frequencies observed for metHb. At the same time, the Raman data provide convincing evidence that native horseradish peroxidase (HRP) and cytochrome  $c'$  are five coordinate.

In the light of these results and of the available data on nonplanar porphyrins, we have reexamined the doming hypothesis. We find that nonplanarity induces a calculable additional lowering of the spin-marker frequencies. While not as influential as core size, the effect is not negligible. A given set of spin-marker frequencies is consistent with a range of values for the core size and the pyrrole tilt angle.

### Experimental Section

Raman spectra were obtained using radiation from either a Spectra Physics 170  $\text{Ar}^+$  laser or a Coherent Radiation 590 dye laser, and a Spex 1401 double monochromator equipped with Ortec/digital photon counting electronics. The spectrometer and photon counting were under control of a Data General Nova 3 computer. Electron para-

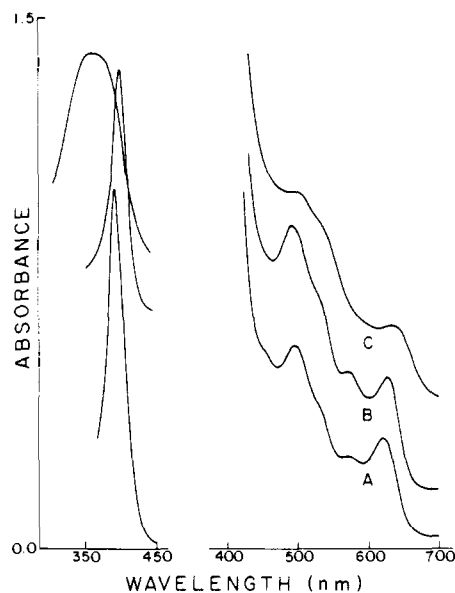


**Figure 1.** Electronic absorption spectra of (A)  $[(\text{Me}_2\text{SO})_2\text{Fe}^{\text{III}}\text{PP}]^+$ , (B) aquometHb, (C)  $\text{ClO}_4\text{Fe}^{\text{III}}\text{PP}$ . All concentrations are 0.1 mM, except for Soret spectra, which were 0.01 mM.

magnetic resonance spectra were recorded on a Varian E-12 spectrometer. Electronic absorption spectra were recorded with a Cary 118 ratio recording spectrophotometer.

Hemin chloride (Sigma) was converted to the dimethyl ester<sup>18</sup> and then to the  $\mu$ -oxo dimer by the method of Sadasivan et al.<sup>19</sup> Hemin perchlorate was prepared by shaking the oxo dimer in methylene chloride with two volumes of 4 M  $\text{HClO}_4$ . The organic phase was separated and anhydrous  $\text{Na}_2\text{SO}_4$  added. The mixture was swirled vigorously for 15 min and filtered. The filtrate was then allowed to stand over anhydrous  $\text{Na}_2\text{SO}_4$  for 5 days. It is extremely important that all water be removed. Traces of water hasten decomposition and interfere with the subsequent formation of the dimethyl sulfoxide ( $\text{Me}_2\text{SO}$ ) complex. Iron(III) octaethylporphyrin perchlorate was prepared as described by Dolphin et al.<sup>22</sup> Methylene chloride was washed first with saturated  $\text{Na}_2\text{CO}_3$ , then twice with water, and dried over  $\text{Na}_2\text{SO}_4$ . Spectral grade  $\text{Me}_2\text{SO}$  (Baker) was purified by standing over 4 Å molecular sieves. Hemoglobin was obtained from lysed human erythrocytes. It was converted to the  $\text{Fe}^{\text{II}}$  form by gentle stirring with a threefold molar excess of potassium ferricyanide, followed by chromatography on a  $3 \times 20$  cm column of Sephadex G-25 coarse, equilibrated with 0.05 M phosphate, pH 6.6 Horse myoglobin was obtained from Miles Research and purified by the method of Hapner et al.<sup>20</sup>

Titration were performed by making additions of titrant ( $\text{Me}_2\text{SO}$ ) directly to a cuvette containing hemin perchlorate in methylene chloride. The absorption spectrum was recorded and the resulting changes in absorption were used to determine the stoichiometry of the reaction by well-established methods.<sup>21</sup> The concentration of the hemin perchlorate solution was determined by titration with imidazole, assuming the formation of the bisimidazole complex to be quantitative.

### Results and Discussion

**Characterization of Bis- $\text{Me}_2\text{SO}$   $\text{Fe}^{\text{III}}$  Hemes.** A methylene chloride solution of  $(\text{ClO}_4^-)\text{Fe}^{\text{III}}\text{PP}$  (PP = protoporphyrin IX dimethyl ester) had a visible absorption spectrum consistent with that reported for the OEP (octaethylporphyrin) analogue.<sup>22</sup> Addition of dimethyl sulfoxide ( $\text{Me}_2\text{SO}$ ) shifted the absorption to a new spectrum as shown in Figure 1. Spectrophotometric titration establishes a 2:1 stoichiometry for the new complex, with quantitative addition of the first  $\text{Me}_2\text{SO}$  molecule. A second  $\text{Me}_2\text{SO}$  molecule is added, with  $K = 23.5 \pm 3.4\text{ M}^{-1}$ . ESR spectroscopy of the solution with excess  $\text{Me}_2\text{SO}$  gave a typical high-spin  $\text{Fe}^{\text{III}}$  spectrum with  $g \approx 6$ . The analogous bis- $\text{Me}_2\text{SO}$   $\text{Fe}^{\text{III}}$ TPP complex has been characterized by La Mar and co-workers,<sup>15</sup> via NMR titration, which

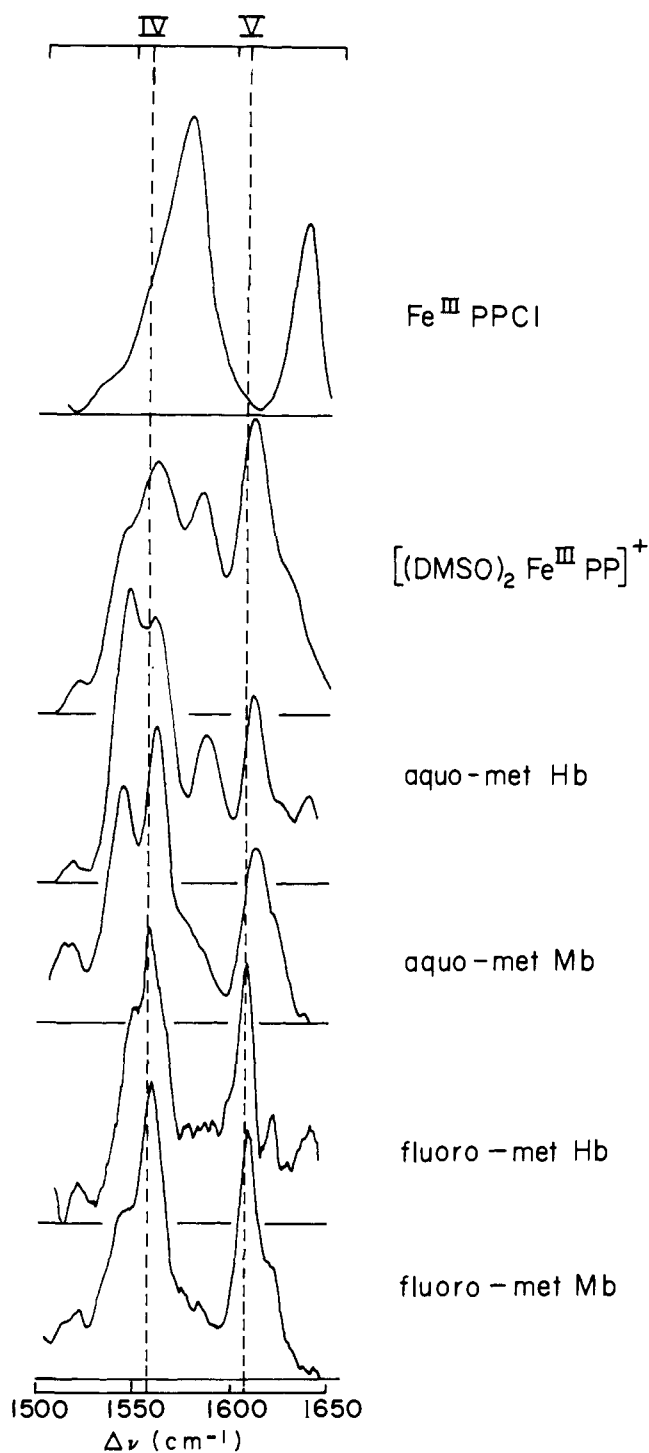


**Figure 2.** Resonance Raman spectra of Fe<sup>III</sup> heme derivatives and proteins obtained with 514.5-nm excitation (except for [(Me<sub>2</sub>SO)<sub>2</sub>Fe<sup>III</sup>PP]<sup>+</sup>, which was excited at 5017 Å). All samples were ~1 mM. Conditions: laser power 300 mW, slit width 3 cm<sup>-1</sup>, scanning speed 3 s/step (0.5 cm<sup>-1</sup>/step). Spectra shown are the accumulation of six complete scans and subjected to a nine-point quintic-quartic smooth. Frequencies are relative to the 1423-cm<sup>-1</sup> line of methylene chloride. The dotted lines mark the band IV and V positions for fluorometHb.

also established the equivalence of the two bound Me<sub>2</sub>SO ligands in the slow exchange temperature range, consistent with the iron atom being in the porphyrin plane. Our solution of (ClO<sub>4</sub><sup>-</sup>)Fe<sup>III</sup>TPP with excess Me<sub>2</sub>SO also displayed a high-spin Fe<sup>III</sup> EPR spectrum. A planar structure has been established by X-ray crystallography for the bis-aquo<sup>16</sup> and bis(tetramethylene sulfoxide)<sup>17</sup> complexes of Fe<sup>III</sup>TPP. It is most likely that high-spin Fe<sup>III</sup> bis-Me<sub>2</sub>SO complexes are also planar.

for porphyrins other than TPP, although this has yet to be confirmed by X-ray crystallography.

**Spin-Marker Raman Frequencies.** Figure 2 shows RR spectra in the 1500–1650-cm<sup>-1</sup> region for [(Me<sub>2</sub>SO)<sub>2</sub>Fe<sup>III</sup>PP]<sup>+</sup>, (Cl<sup>-</sup>)Fe<sup>III</sup>PP, and aquo- and fluorometHb (hemoglobin) and Mb (myoglobin). The observed frequencies and polarizations are given in Table I. Table II lists the frequencies of the three bands, labeled II, IV, and V, which have been found to be sensitive to variations in the spin state of the iron atom.<sup>2,8</sup> Included in this table are representative examples of other spin and oxidation states, and a series of high-spin heme protein derivatives. The last column contains values of C<sub>1</sub>-N, the porphyrin center to pyrrole nitrogen distance, which is a measure of the porphyrin core size. Some of the listed distances are obtained from crystal structures for porphyrins, including TPP, other than those for which the Raman frequencies are given. Structural parameters do not seem to vary significantly, however, with alterations in the porphyrin substituents.<sup>9</sup> For comparison of vibrational frequencies it is essential that the methine bridges have hydrogen atoms and that the β-pyrrole positions have carbon substituents.<sup>2,8</sup>

Table II makes it evident that the general correlation of the band IV frequency with core size observed by Spaulding et al.<sup>11</sup> holds for all the iron hemes, and it also holds for bands II and V (although the low-spin Fe<sup>II</sup> frequencies are exceptional—see below). For comparable spin states the Fe–pyrrole bonds are slightly longer for Fe<sup>II</sup> than Fe<sup>III</sup>, reflecting the reduced effective charge, although the shortest bonds are found for four-coordinated (intermediate-spin) Fe<sup>II</sup>, the effective charge being increased by the absence of any axial ligands.<sup>13</sup> High-spin hemes have longer Fe–pyrrole bonds than low-spin hemes because of the partial occupancy of the antibonding d<sub>x<sup>2</sup>-y<sup>2</sup></sub> orbitals. For five-coordinate high-spin hemes this repulsion is partially relieved by the iron atom moving out of the porphyrin plane in the direction of the axial ligand. There is also a significant expansion of the porphyrin core, however. When high-spin Fe<sup>III</sup> is forced into the plane by two equivalent axial ligands the porphyrin core expands further.

[(Me<sub>2</sub>SO)<sub>2</sub>Fe<sup>III</sup>PP]<sup>+</sup> gives RR frequencies (Table I) which are close to those found in other iron TPP complexes.<sup>23</sup> Vibrational coupling with ring substituents produces a substantially altered normal mode pattern for TPPs, and clear-cut spin- and oxidation-state markers are not observed.<sup>23</sup> There are, however, two polarized bands, at ~1550 and ~1360 cm<sup>-1</sup> (also one at ~390 cm<sup>-1</sup>, in a frequency region not included in the present study) which vary systematically with both oxidation and spin state.<sup>23</sup> They are found at 1568 and 1370 cm<sup>-1</sup> for low-spin Fe<sup>III</sup>, and at 1555 and 1366 cm<sup>-1</sup> for five-coordinate high-spin Fe<sup>III</sup>. The present data place the six-coordinate high-spin Fe<sup>III</sup> frequencies at 1550 and 1360 cm<sup>-1</sup>, below those of five-coordinate Fe<sup>III</sup>, as expected from core expansion.

**Insensitivity to Fe Out-of-Plane Displacement. MetHb and Mb.** Spaulding et al.<sup>11</sup> proposed that, if C<sub>1</sub>-N could be determined from the band IV frequency, then the distance of the iron atom from the plane of the four nitrogen atoms could be calculated by triangulation, assuming that the Fe–pyrrole distance for high-spin Fe<sup>III</sup> or Fe<sup>II</sup> is constant. The crystal structure of the planar high-spin Fe<sup>III</sup>TPP derivatives<sup>16,17</sup> shows this assumption to be incorrect. Their Fe–pyrrole distances are shorter than those found for five-coordinate high-spin Fe<sup>III</sup> complexes.<sup>9</sup> Scholler and Hoffman<sup>24</sup> have proposed a different method for estimating the frequency shift accompanying out-of-plane displacement.

The present RR data on metHb and Mb, taken together with the X-ray crystallographic results,<sup>14,25</sup> establish that *core expansion and iron out-of-plane displacement are unrelated*, at least for six-coordinate high-spin Fe<sup>III</sup>. The frequencies of aquometHb and Mb are the same despite substantially dif-

Table I. Raman Frequencies (cm<sup>-1</sup>) of Six-Coordinate Ferric Hemes

|  |           |                   |           |           |           |                   |
|--|-----------|-------------------|-----------|-----------|-----------|-------------------|
| aquometHb  | 1481 (p)  | 1549 <sup>a</sup> | 1561 (ap) | 1583 (p)  | 1610 (dp) | 1623 <sup>a</sup> |
| aquometMb  | 1482 (p)  | 1546              | 1562 (ap) | 1582 (p)  | 1611 (dp) | 1626              |
| fluorometHb  | 1482 (p)  | 1546              | 1556 (ap) | 1583 (p)  | 1608 (dp) | 1621              |
| fluorometMb  | 1482 (p)  | 1544              | 1557 (ap) | 1583 (p)  | 1609 (dp) | 1619              |
| [(Me <sub>2</sub> SO) <sub>2</sub> Fe <sup>III</sup> PP] <sup>+</sup>  | 1475 (p)  | 1545              | 1560 (ap) | 1583 (p)  | 1610 (dp) | 1628              |
| [(Me <sub>2</sub> SO) <sub>2</sub> Fe <sup>III</sup> OEP] <sup>+</sup> | 1481 (p)  | 1552              | 1563 (ap) | 1577 (p)  | 1613 (dp) | 1629              |
| [(Me <sub>2</sub> SO) <sub>2</sub> Fe <sup>III</sup> TPP] <sup>+</sup> | 1333 (ap) | 1360 (p)          | 1491 (p)  | 1508 (ap) | 1550 (p)  | 1597 (p)          |

<sup>a</sup> These bands appear as shoulders, and are of uncertain polarization.

Table II. Raman Frequencies (cm<sup>-1</sup>) of Structure-Sensitive Bands and C<sub>1</sub>-N Distances (Å)

|  | II   | IV   | V    | C <sub>1</sub> -N    | ref           |
|--|------|------|------|----------------------|---------------|
| Fe <sup>II</sup> intermediate spin Fe <sup>II</sup> MP   | 1506 | 1589 | 1642 | 1.972 <sup>13</sup>  | 8             |
| Fe <sup>III</sup> low-spin [(1m) <sub>2</sub> Fe <sup>III</sup> MP] <sup>+</sup>                     | 1505 | 1584 | 1640 | 1.989 <sup>54a</sup> | 8, 11         |
| Fe <sup>II</sup> low-spin [(1m) <sub>2</sub> Fe <sup>II</sup> PP]                                    | 1491 | 1583 | 1617 | 2.004 <sup>54b</sup> | 8, 11         |
| Fe <sup>III</sup> high-spin 5c ClFe <sup>III</sup> PP  | 1495 | 1572 | 1632 | 2.019 <sup>9</sup>   | 11            |
| Fe <sup>III</sup> high-spin 6c [(Me <sub>2</sub> SO) <sub>2</sub> Fe <sup>III</sup> PP] <sup>+</sup> | 1475 | 1560 | 1610 | 2.045 <sup>17</sup>  | this work, 11 |
| Fe <sup>III</sup> high-spin 6c (Me <sub>2</sub> SO) <sub>2</sub> Fe <sup>III</sup> OEP <sup>+</sup>  | 1481 | 1563 | 1613 |                      | this work     |
| Fe <sup>II</sup> high-spin 2-MelmFe <sup>II</sup> MP   | 1472 | 1558 | 1606 | 2.044 <sup>56</sup>  | 8, 11         |
| high-spin Fe <sup>II</sup> proteins:   |      |      |      |                      |               |
| dcoxyHb  | 1473 | 1552 | 1607 |                      |               |
| Fe <sup>II</sup> HRP   | 1472 | 1553 | 1605 |                      |               |
| high-spin Fe <sup>III</sup> proteins   |      |      |      |                      |               |
| aquometHb  | 1481 | 1561 | 1610 |                      | this work     |
| aquometMb  | 1482 | 1562 | 1611 |                      | this work     |
| fluorometHb  | 1482 | 1556 | 1608 |                      | this work     |
| fluorometMb  | 1482 | 1557 | 1609 |                      | this work     |
| fluoro-HRP   | 1482 | 1555 | 1608 |                      | 32            |
| native HRP   | 1500 | 1575 | 1608 |                      | 32            |
| cytochrome c' (pH 6.9)   | 1500 | 1578 | 1637 |                      | 42            |
| cytochrome c' (pH 10.3)  | 1496 | 1573 | 1633 |                      | 42            |

ferent Fe-mean heme plane displacements: 0.40 Å for metMb<sup>25</sup> and 0.23 and 0.07 Å for the β and α chains of metHb.<sup>14</sup> Moreover, the metHb RR spectrum (Figure 2) shows no detectable splitting of the spin-marker band reflecting the chain inequivalence. The frequencies for both proteins are quite close to those of [(Me<sub>2</sub>SO)<sub>2</sub>Fe<sup>III</sup>PP]<sup>+</sup> (Table II), but substantially lower than those of (Cl<sup>-</sup>)Fe<sup>III</sup>PP or other five-coordinate high-spin hemes. It appears that six coordination per se is the main determinant of the spin-marker frequencies, and, by implication, of the core expansion.

This conclusion implies that the porphyrin core size is not determined by the size of the high-spin ferric ion itself, but rather by interactions with the axial ligands. Recent ab initio calculations by Olafson and Goddard<sup>26</sup> and semiempirical calculations by Warshel<sup>27</sup> point to the importance of nonbonded repulsions between the axial ligands and the pyrrole nitrogen atoms in the structure and energetics of the heme group. For five-coordinate hemes, it appears<sup>26</sup> that the out-of-plane displacement of the iron atom depends on the optimization of iron-ligand bonding within a coordination geometry that is fixed by the axial ligand-pyrrole interactions. This ordering of energies is likely to hold also for six-coordinate high-spin hemes. When the axial ligands are equivalent, then the iron atom is constrained to lie in the heme plane. The potential curve for out-of-plane displacement is likely to be relatively flat, however.<sup>27</sup> When the ligands are not equivalent, the position of the iron atom can be expected to depend on the relative bond strengths to the axial ligands and their nonbonded interactions with the pyrrole rings. The balance of these forces may provide for considerable flexibility in the axial geometry. It is of interest in this connection that in (py)(Cl<sup>-</sup>)Mn<sup>III</sup>TPP<sup>28</sup> the Mn atom is displaced toward the chloride ion and the long bond is to pyridine. Although pyridine is a stronger field ligand, this is outweighed for the high-spin Mn<sup>3+</sup> ion by the negative charge on Cl<sup>-</sup>.

metHb and metMb have the same axial ligand set, imidazole and water. For the metHb α chains the axial forces are evenly

balanced and the iron atom is only 0.07 Å from the mean heme plane. For the β chains and for metMb tertiary forces apparently pull on the imidazole, the out-of-plane displacement increasing to 0.23 and 0.42 Å respectively. Presumably the imidazole-pyrrole repulsion is weakened, but the water-pyrrole repulsion must be strengthened by the same amount since the RR frequencies show the porphyrin core size to remain constant. The overall change in the energy of the heme complex may be quite small. It must be sufficient, however, to account for the lower fraction of low-spin forms in metMb complexes relative to the corresponding metHb complexes.<sup>29</sup> As Ladner et al.<sup>14</sup> have pointed out, this trend is consistent with the larger out-of-plane displacement observed for metMb. The potential curve for out-of-plane displacement is expected to be steeper for low-spin than for high-spin Fe<sup>III</sup> because of the greater bond directionality of the former. Consequently, protein forces favoring out-of-plane displacement will raise the energy of the low-spin form relative to the high-spin form.

The fluoride complexes of metHb and Mb (Figure 2 and Table II) show essentially the same band II and V frequencies as do the aquo complexes, but band IV is 5 cm<sup>-1</sup> lower. A difference Fourier map of fluoro- vs. aquo metHb, at 2.8-Å resolution, shows some tertiary structure alterations but no significant changes in the heme structure.<sup>30</sup> The decreased band IV frequency may reflect these tertiary alterations, or it may result from increased nonbonded interactions of the anionic fluoride ligands.

**Five Coordination in Horseradish Peroxidase and Cytochrome c'.** As noted previously,<sup>8,31</sup> the spin-marker frequencies for native horseradish peroxidase (HRP, which contains high-spin Fe<sup>III</sup>), 1500, 1575, and 1630 cm<sup>-1</sup> for bands II, IV, and V, are close to those of five-coordinate Fe<sup>III</sup> porphyrins, rather than those of metHb or metMb (see Table II). In view of the present evidence that the metHb and metMb frequencies are characteristic of six-coordinate high-spin Fe<sup>III</sup> porphyrins, the HRP frequencies clearly point to five coordination for the native form of the protein. This inference is consistent with the

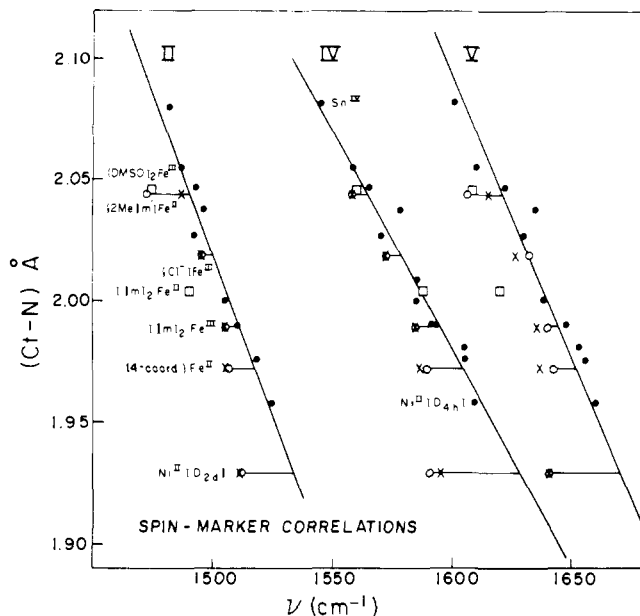


**Figure 3.** Frequency vs.  $C_1-N$  plots for bands II, IV, and V. The filled circles, which are used to establish the straight lines, are data taken from ref 11. Open circles are data points for the indicated nonplanar porphyrins:<sup>8,11</sup> (2-Melm)Fe<sup>II</sup>MP, (Cl<sup>-</sup>)Fe<sup>III</sup>MP, [(1m)<sub>2</sub>Fe<sup>II</sup>MP]<sup>+</sup>, Fe<sup>II</sup>MP, and Ni<sup>II</sup>(OEP) ( $D_{2d}$ ), with structural data taken from ref 56, 59, 54, 13, and 53, respectively. Crosses are frequencies calculated via eq 2. Open squares are planar porphyrins, (1m)<sub>2</sub>Fe<sup>II</sup>(MP) and [(Me<sub>2</sub>SO)Fe<sup>III</sup>PP]<sup>+</sup>, which give discrepant band II and V frequencies, as discussed in the text.

NMR relaxation data presented by Lanir and Shejter,<sup>32</sup> which establish that the native HRP heme group does *not* have an exchangeable water molecule bound to it. A five-coordinate heme would have no bound water if the fifth ligand were provided by the protein. The identity of the fifth ligand is uncertain, but imidazole is implicated by ultraviolet difference spectra<sup>33</sup> and by the ESR hyperfine splitting pattern in the nitrosyl complex of reduced HRP.<sup>34</sup>

While solvent water does not bind to HRP, exogenous anionic ligands can be made to bind. The fluoride complex gives RR frequencies<sup>31</sup> which are the same as those of fluorometHb (Table II) implying six coordination, while the CN<sup>-</sup> complex is low spin and six coordinate.<sup>31</sup> However, anion binding is always accompanied by the binding of a proton to the protein.<sup>35</sup> This has been interpreted by George and co-workers<sup>36</sup> as requiring displacement of a deprotonated ligand, such as tyrosine phenolate, from the heme iron atom. The present data, pointing to five coordination, suggest that the deprotonated group is not actually bound to the iron atom, but is close enough to block access to it. Alternatively a deprotonated distal group *is* bound to the heme iron, but the bond to the proximal imidazole is broken, being formed upon binding of exogenous ligands which displace the distal group. (The spectroscopic evidence bearing on imidazole coordination does not establish an intact bond in native HRP). In view of the flexibility of high-spin Fe<sup>III</sup> with respect to the porphyrin core (inversion of five-coordinate Fe<sup>III</sup> through the porphyrin is known to occur on a time scale of  $\sim 10^{-2}$  s<sup>37</sup>) switching of endogenous ligands is not implausible. Just this structure has been found by Pulsinelli et al.<sup>38</sup> in the Hb M Boston valency hybrid, the Fe<sup>3+</sup> ion of the mutant  $\alpha$  chains being bound to the distal tyrosine and not to the proximal imidazole. It would be of interest to examine the RR spectrum of this hybrid, since we expect the contribution from the Fe<sup>III</sup> hemes to resemble native HRP rather than metHb.

Spaulding et al.<sup>11</sup> reported that the benzhydroxamate complex of HRP gives a band IV frequency of 1566 cm<sup>-1</sup>,

intermediate between the frequencies observed for the fluoride (1555 cm<sup>-1</sup>) and for native HRP (1575 cm<sup>-1</sup>). It may be that binding of benzhydroxamate induces a weak axial interaction on the distal side, either with itself or with solvent water. The latter possibility is suggested by the ESR study of the hydroxamate complex by Gupta and Schonbaum,<sup>39</sup> which established a definite hyperfine splitting by <sup>17</sup>OH<sub>2</sub> solvent, although the extent of the splitting (1 G) was much smaller than that observed for metMb (18 G).<sup>40</sup>

Another Fe<sup>III</sup> heme protein that shows a five-coordinate RR pattern is cytochrome *c'* from *Rhodospseudomonas palustris*.<sup>41,42</sup> In this case the heme iron atom is not accessible to exogenous ligands in the oxidized form of the protein.<sup>43</sup> The magnetic moment is intermediate between low- and high-spin Fe<sup>III</sup>,<sup>44</sup> but the Raman data rule out a spin-state mixture.<sup>41,42</sup> EPR spectroscopy has confirmed that the spin state itself is intermediate.<sup>45</sup> Also HRP, although high spin, is believed to be poised at the edge of an intermediate spin state, which is stabilized at low temperature.<sup>46</sup>

In this connection it is of considerable interest that the perchlorate complexes of Fe<sup>III</sup>OEP<sup>22</sup> and Fe<sup>III</sup>TPP<sup>16</sup> have been shown to be intermediate spin. The crystal structure of the TPP complex<sup>16</sup> shows it to be five coordinate, but the Fe-pyrrole bonds are nearly as short as those found in low-spin Fe<sup>III</sup> porphyrin consistent with depopulation of the antibonding  $d_{z^2-y^2}$  orbital.<sup>16</sup> Perchlorate is a very weak ligand field, and thus it appears that, if the axial field is weakened sufficiently, then the intermediate-spin state is stabilized. This suggests that a protein containing a five-coordinate Fe<sup>III</sup> heme can convert from high to intermediate spin by stretching the Fe axial ligand bond. The EPR work of Maltempo et al.<sup>45</sup> suggests that the transition is continuous, rather than discrete, since they find a quantum admixture of high- and intermediate-spin contributions, i.e., a state "intermediate" between  $S = 5/2$  and  $S = 3/2$ .

The structural parameters for (ClO<sub>4</sub><sup>-</sup>)Fe<sup>III</sup>TPP<sup>16</sup> indicate that stabilization of the intermediate-spin state should be accompanied by a contraction of  $C_1-N$ , and therefore an increase in the spin-marker RR frequencies. (We were unfortunately unable to obtain RR spectra for perchlorate adducts because of their instability upon laser excitation.) Lowering the pH of Fe<sup>III</sup> cytochrome *c'* from 10.3 to 6.9 decreases the magnetic moment appreciably<sup>44</sup> (reflecting a decreased  $S = 5/2$  contribution to the spin state<sup>45</sup>) and also shifts the spin-marker RR frequencies<sup>41</sup> *up* from typical five-coordinate values toward the values observed for low-spin Fe<sup>III</sup> (Table II). We interpret the change in cytochrome *c'* structure between pH 10.3 and 6.9 as a weakening of the bond to the fifth ligand, accompanied by a strengthening of the Fe-pyrrole bonds, and a decrease in  $C_1-N$ .

**Core Expansion and Pyrrole Tilting. A. Linear Dependence on  $C_1-N$ .** The present results establish that the correlation between the spin-marker frequencies and  $C_1-N$  discovered by Spaulding et al.<sup>11</sup> for band IV applies in a general way to iron porphyrin complexes. Huong and Pommier<sup>47</sup> have plotted the band IV and V frequencies against  $C_1-N$  for a large number of metalloporphyrins, and have found well-behaved linear relationships:

$$\nu = K(A - d) \text{ cm}^{-1} \quad (1)$$

where  $d$  is the  $C_1-N$  distance and the parameters  $K$  (cm<sup>-1</sup>/Å) and  $A$  (Å) have the values 555.6 and 4.86 for band IV and 423.7 and 5.87 for band V. Scholler and Hoffman<sup>24</sup> found a similar straight line for band IV. These lines are drawn in Figure 3 along with a third line which we have constructed to fit the available data for band II, with  $K = 375.5$  and  $A = 6.01$ .

The filled circles in Figure 3 are data points for a variety of

porphyrins with differing  $C_1-N$ . Most of them fall satisfactorily on the lines. For  $(1m)_2Fe^{II}MP$ ,  $(2Melm)Fe^{II}MP$ , and  $(Me_2SO)_2Fe^{III}PP^+$ , the frequencies fall on the band IV line, but significantly ( $15-20\text{ cm}^{-1}$ ) below the lines for bands II and V. These latter bands have previously been noted as being sensitive to oxidation as well as spin state in iron porphyrins.<sup>2,8</sup>

Bands II, IV, and V show substantial ( $4-11\text{ cm}^{-1}$ ) shifts upon methine deuteration, whereas other bands in the  $1350-1650\text{-cm}^{-1}$  region do not.<sup>8,11</sup> The three normal modes are thus assignable primarily to the stretching of the methine bridge bonds. The inverse correlation with  $C_1-N$  is plausibly linked to the decrease in the associated force constant when the methine bridges are stretched and bent to accommodate core expansion. The lowered band II and V frequencies observed for low-spin  $Fe^{II}$  reflect its propensity for back-donation of  $d_\pi$  electrons to  $\pi^*$  orbitals of the porphyrin ring; the frequencies are raised when the axial imidazole ligands are replaced by good  $\pi$  acceptors, which compete with the porphyrin for the iron  $d_\pi$  electrons. Because the lowest porphyrin  $\pi^*$  orbital has nodes between the nitrogen atoms and the methine carbon atoms,<sup>48</sup> back-donation is not expected to influence directly the methine bridge force constants, but rather those internal to the pyrrole ring. The internal coordinates are mixed in the normal modes,<sup>10,49-51</sup> however, and the influence of back-donation on the band II and V frequencies may be a reflection of the extent of mixing. The lack of sensitivity of band IV may be related to the fact that the mode is of  $A_{2g}$  symmetry, and stretching of the pyrrole  $C_\beta-C_\beta$  pyrrole bonds cannot contribute to the  $A_{2g}$  block. We are unable to explain the anomalously low band II and V frequencies for  $[(Me_2SO)_2Fe^{III}PP]^+$  or for  $(2Melm)Fe^{II}MP$ , however.

**B. Doming and Ruffling.** The open circles in Figure 3 are data points for nonplanar porphyrins. They fall systematically below the lines, and we attribute the deviations to lowering of the methine bridge bond-stretching force constants resulting from reduction in  $\pi$  overlap when the pyrrole rings are tilted out of the mean plane. There are two kinds of pyrrole tilt which are observed in metalloporphyrin structures and have been discussed by Hoard.<sup>9</sup> They are shown diagrammatically in Figure 4. In ruffled porphyrins the pyrrole rings swivel about the metal-nitrogen bonds, reducing the symmetry to  $D_{2d}$ . This leaves a square-planar  $MN_4$  array, but permits a shortening of the  $M-N$  bond.<sup>9</sup> The ruffled structure is observed for metals whose  $M-N$  bonds are shorter than  $C_1-N$  for an unconstrained planar porphyrin, estimated by Hoard<sup>9</sup> to be  $2.01\text{ \AA}$ . An interesting example is provided by NiOEP, which can be crystallized in two forms. The triclinic modification<sup>52</sup> contains a planar porphyrin, with  $Ni-N = 1.958\text{ \AA}$ , while the orthorhombic form<sup>53</sup> contains a ruffled porphyrin with  $Ni-N = 1.929\text{ \AA}$ . There is evidently a close balance between loss of  $\pi$  conjugation in the ruffled structure and loss of  $Ni-N$  bond strength in the planar structure, which can be shifted by crystal packing forces. Spaulding et al.<sup>11</sup> observed that the two forms gave distinctly different RR spectra. While band IV was at the frequency predicted by the  $C_1-N$  correlation for the planar form, it decreased appreciably in the ruffled form, contrary to the  $C_1-N$  correlation. Ruffled structures are also found for four-coordinate  $Fe^{II}TPP$ <sup>13</sup> and for  $[(1m)_2Fe^{II}OEP]Cl$ ,<sup>54</sup> in both of which the  $Fe-N$  distance is significantly shorter than  $2.01\text{ \AA}$ .

A second type of pyrrole tilting is found in domed porphyrins, which are usually five coordinate.<sup>9</sup> The metal atom lies above the porphyrin plane and this motion is followed by the pyrrole rings, which swivel about the methine bridge bonds causing the nitrogen plane,  $P_N$ , to lie above the mean plane of the porphyrin,  $P_C$ . The symmetry reduces to  $C_{4v}$ .

**C. A Quantitative Model.** As demonstrated by the crosses in Figure 3, the frequencies of the nonplanar porphyrins are

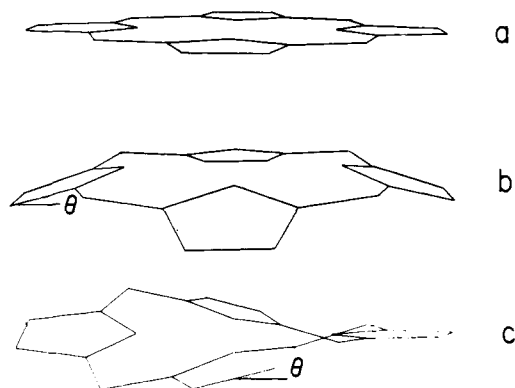


**Figure 4.** Perspective drawings for (a) planar, (b) domed, and (c) ruffled porphyrin skeletons from  $\sim 10^\circ$  above.  $\theta$  is the angle by which the pyrroles tilt out of the mean porphyrin plane.

accurately calculated by the equation

$$\nu = (K^2(A - d)^2 \cos^2 \phi + B^2 \sin^2 \phi)^{1/2} \quad (2)$$

where the parameter  $B$  ( $\text{cm}^{-1}$ ) is 1332, 1347, and 1438 for bands II, IV, and V.  $\phi$  is the methine bridge dihedral angle between the  $N-C_\alpha-C_m$  and  $C_\alpha-C_m-C_\alpha$  planes. Its calculation from the crystallographic data is described in Appendix A. For planar porphyrins  $\phi = 0$ , and eq 2 reduces to eq 1.

The derivation of eq 2 is given in Appendix B. It is based on a model of uncoupled normal modes associated solely with  $C_\alpha-C_m$  bond stretching, with force constants made up of  $\sigma$  and  $\pi$  contributions,  $F_\sigma$  and  $F_\pi$ . The influence of core expansion and nonplanarity is carried by  $F_\pi$ . From the empirically determined parameters,  $K$ ,  $A$ , and  $B$ , for bands II, IV, and V, respectively, this model gives  $F_\sigma = 7.7$ ,  $5.4$ , and  $6.2\text{ mdyn/\AA}$  and  $F_\pi = 2.1$ ,  $1.3$ , and  $1.8\text{ mdyn/\AA}$  for an unconstrained porphyrin with  $C_1-N = 2.01\text{ \AA}$ .<sup>9</sup> Neglect of coupling with other normal modes could well account for the differences among the three estimates.

Taken together, however, these values are not far from what one might expect for methine bridges of bond order  $\sim 1.5$ , considering that bond stretching force constants are roughly 5 and  $10\text{ mdyn/\AA}$  for single and double carbon-carbon bonds.<sup>58</sup> They suggest that the present model of combined core expansion and pyrrole tilting effects is not completely unreasonable, and could serve as a starting point for a more sophisticated treatment.

While the good account of the data given by eq 2 is satisfying, it also establishes that there is no unique way of using the RR frequencies to determine either core size or pyrrole tilt in porphyrins of unknown structure. Each set of frequencies is consistent with a range of  $C_1-N$  and  $\theta$  values. In Figure 5 the loci of these values are shown for different values of the band IV frequency. The curves are quite flat for moderate values of  $\theta$ , demonstrating that core size is the main determinant of the vibrational frequencies. If severe tilting were to occur, however, it would produce the same lowering of the frequencies as would modest core expansion.

## Conclusions

At present there is no RR evidence to suggest significant protein-induced distortion of the porphyrin core in the heme proteins so far studied. In all cases their derivatives can be modeled with reasonable accuracy by simple porphyrin complexes. It is clear that the number of axial ligands and their properties are the main determinants of the porphyrin vibrational frequencies. Their influence on the spin-marker frequencies is related to porphyrin core expansion through steric interactions (although electronic effects are also evident for low-spin  $Fe^{II}$ ). In addition porphyrin ruffling or doming

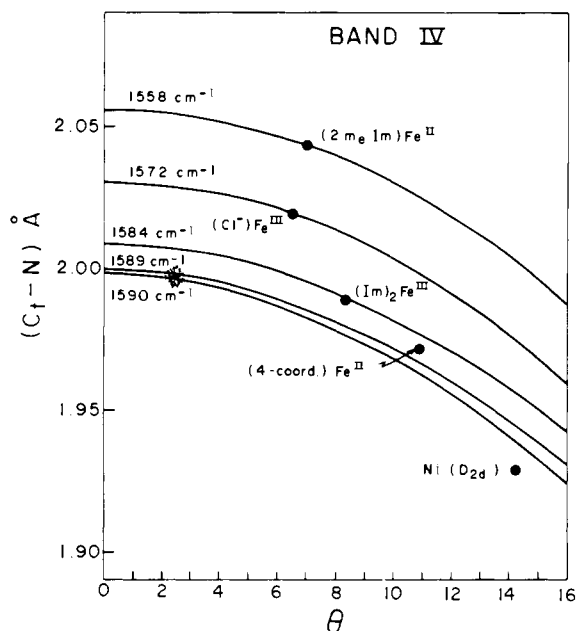


**Figure 5.** Loci of  $C_1-N$  distance and pyrrole tilt angles, allowed by eq 2 and the geometric relations in the Appendix for the band IV frequencies of the indicated complexes. Symbols and structural references as in Figure 3.

have subsidiary effects on the frequencies. Since domed porphyrins (five-coordinate  $Fe^{III}$  and  $Fe^{II}$ ) show essentially the same frequencies whether inside a heme protein or not, there is not reason to think that proteins exert a marked effect on doming, as had been suggested for metHb and metMb.<sup>8</sup>

It should be emphasized, however, that the present treatment is highly simplified. There are certainly more distortion coordinates that might play a role than a single core size and a single methine dihedral angle. We do not understand at present why both  $(2MeIm)Fe^{II}MP$  and  $[(Me_2SO)_2Fe^{III}PP]^+$  show the expected frequency for band IV, but low values for bands II and V, or why fluorometHb and Mb shows a decrease in band IV, but not bands II and V, relative to aquometHb and Mb or to  $[(Me_2SO)_2Fe^{II}PP]^+$ . This behavior suggests additional methine bridge influences which distinguish among bands II, IV, and V.

**Acknowledgment.** We thank Drs. W. R. Scheidt, C. A. Reed, and B. M. Hoffman for communicating results of their work prior to publication. This work was supported by NIH Grant HL 12526.

#### Appendix A. Methine Dihedral Angles

Pyrrole tilting produces a rotation about the  $C_\alpha C_m$  bonds, which is equal and opposite for the two bonds at each methine bridge. The difference between domed and ruffled porphyrins is that pairs of rotations have the same phase sequence for each successive methine bridge in the domed structure, but alternate in phase in the ruffled structure. The connection between the  $C_\alpha C_m$  rotation (dihedral) angles,  $\phi$ , and the pyrrole tilt angle,  $\theta$ , is given by the following trigonometric relations:

$$\begin{aligned} \text{doming: } \phi_d &= \sin^{-1}(\tan \psi_d \tan(\gamma/2)) \\ &\quad + \sin^{-1}(\tan \psi_d \tan \tau) \\ \text{ruffling: } \phi_r &= \sin^{-1}(\tan \psi_r \tan(\gamma/2)) \\ &\quad - \sin^{-1}(\tan \psi_r \cot \tau) \end{aligned}$$

The angles  $\gamma$  and  $\tau$  are defined by

$$\begin{aligned} \gamma &= \angle(C_\alpha C_m C_\alpha) \\ \tau &= \angle(C_m C_\alpha N) - \frac{1}{2}\angle(C_\alpha N C_\alpha) \end{aligned}$$

and  $\theta$  is the angle of tilt of the pyrrole rings with respect to the mean porphyrin plane. In the present model, the pyrrole rings are assumed to be coplanar with the adjacent  $C_m$  atoms, and the methine bridge angles are given by

$$\text{doming: } \cos \gamma = |1.0 - (\sin \tau + \cos \tau \cos \theta)^2|$$

$$\text{ruffling: } \cos \gamma = |1.0 - (\cos \tau + \sin \tau \cos \theta)^2|$$

Actual crystal structures do not necessarily conform strictly to the idealized  $C_{4v}$  or  $D_{2d}$  symmetries assumed for domed and ruffled porphyrins. An average tilt angle,  $\theta_{av}$ , can be calculated, from the reported atomic displacements from the mean plane.<sup>52</sup> For domed porphyrins  $\theta_{av}$  is calculable from the reported  $P_N-P_C$  distance.<sup>55</sup> For porphyrin structures we have examined the angle  $\tau$  is essentially constant,  $72.5 \pm 0.5^\circ$ . The parameters  $\psi_d$  and  $\psi_r$  are given by

$$\sin \psi_d = \cos \tau \sin \theta$$

$$\sin \psi_r = \sin \tau \sin \theta$$

#### Appendix B. Interpretation of Equation 2

The vibrational secular equation is given by

$$|GF - \lambda| = 0 \quad (3)$$

where  $G$  and  $F$  are the kinetic and potential energy matrices<sup>57</sup> and

$$\lambda = 4\pi^2 c^2 \nu^2 \quad (4)$$

( $c$  is the velocity of light and  $\nu$  is expressed in  $cm^{-1}$ ). For the present model we assume that the normal modes are not coupled and that the solution

$$\lambda = GF \quad (5)$$

applies to each of them,  $G$  and  $F$  being the appropriate (diagonal) matrix elements. The normal mode force constant,  $F$ , may be arbitrarily divided into contributors from  $\sigma$  and  $\pi$  bonding:

$$F = F_\sigma + F_\pi \quad (6)$$

It seems reasonable to attribute tilting effects to  $F_\pi$  which should vary as some function of  $\cos \phi$ . We select

$$F_\pi = F_\pi^0 \cos^2 \phi \quad (7)$$

because it gives reasonable values of  $F_\pi^0$ ; the fact that there are actually two adjacent dihedral angles at each methine bridge, which are equal but have opposite senses, lends some plausibility to the use of  $\cos^2 \phi$  rather than  $\cos \phi$ . We also choose to place the influence of core expansion on  $F_\pi^0$ . The reason for this is that the experimental data given in Figure 3 indicate that the effect of ring tilting decreases with increasing core size; this interaction can be taken into account by allowing the frequency decrease on core expansion to reflect an associated decrease in  $F_\pi$ , keeping  $F_\sigma$  constant.

Combining 1, 4, 5, and 6 we have for planar porphyrins that

$$K^2(A - d)^2 = G'(F_\sigma + F_\pi^0) \quad (8)$$

where  $G' = G/4\pi^2 c^2$ , and that

$$F_\pi^0 = K^2(A - d)^2/G' - F_\sigma \quad (9)$$

With the above assumptions the relationship for tilted porphyrins should be

$$\nu = (G'(F_\sigma + F_\pi^0 \cos^2 \phi))^{1/2} \quad (10)$$

which, on substitution of eq 9, becomes

$$\nu = (K^2(A - d)^2 \cos^2 \phi + G'F_\sigma \sin^2 \phi)^{1/2} \quad (11)$$

Equation 11 gives eq 2 with the identification  $B \equiv \sqrt{G'F_\sigma}$ .

If the normal modes consisted solely of  $C_{\alpha}-C_m$  stretching, then the  $G$  matrix elements would simply be  $(1 + 2 \sin^2 \gamma)/m_c$  ( $m_c$ , the carbon mass, is 12) for both band IV and V (the  $A_{2g}$  and  $B_{1g}$  symmetries both involve out-of-phase stretching of adjacent  $C_{\alpha}-C_m$  bonds), and  $(1 + 2 \cos^2 \gamma)/m_c$  for band II ( $A_{1g}$ , in phase), where  $\gamma$  is the  $C_{\alpha}C_mC_{\alpha}$  angle,  $124^\circ$ . These values of  $G$  were combined with the empirically determined values of  $B$  to calculate the  $F_\sigma$  values given in the text. Equation 9 gives  $F_{\pi^0}$ , which depends on  $d$ ; the estimate of  $2.01 \text{ \AA}$  for an unconstrained porphyrin is due to Hoard.<sup>9</sup>

## References and Notes

- (1) T. G. Spiro, *Biochim. Biophys. Acta*, **416**, 169 (1975), and references cited therein.
- (2) T. G. Spiro and T. C. Strekas, *J. Am. Chem. Soc.*, **96**, 338 (1974).
- (3) F. Adar and M. Erecinska, *Arch. Biochem. Biophys.*, **165**, 570 (1974).
- (4) F. Adar and T. Yonetani, *Biochim. Biophys. Acta*, **502**, 80 (1978).
- (5) (a) T. Yamamoto, G. Palmer, D. Gill, I. Salmeen, and L. Rimai, *J. Biol. Chem.*, **248**, 5211 (1973); (b) I. Salmeen, L. Rimai, and G. Babcock, *Biochemistry*, **17**, 800 (1978).
- (6) (a) P. M. Champion and I. C. Gunsalus, *J. Am. Chem. Soc.*, **99**, 2000 (1977); (b) P. M. Champion, I. C. Gunsalus, and G. C. Wagner, *ibid.*, **100**, 3743 (1978).
- (7) (a) T. Kitagawa, T. Iizuka, M. Saito, and Y. Kyogoku, *Chem. Lett.*, 849 (1975); (b) Y. Ozaki, T. Kitagawa, Y. Kyogoku, T. Iizuka, and Y. Ishimura, *J. Biochem. (Tokyo)*, **80**, 1447 (1976); (c) T. Kitagawa, M. Abe, Y. Kyogoku, H. Ogoshi, H. Sugimoto, and Z. Yoshida, *Chem. Phys. Lett.*, **48**, 55 (1977).
- (8) T. G. Spiro and J. M. Burke, *J. Am. Chem. Soc.*, **98**, 5482 (1976).
- (9) J. L. Hoard in "Porphyrins and Metalloporphyrins", K. M. Smith, Ed., American Elsevier, New York, 1975, pp 317-376.
- (10) (a) P. Stein, J. M. Burke, and T. G. Spiro, *J. Am. Chem. Soc.*, **97**, 1304 (1975); (b) T. G. Spiro and T. C. Strekas, *Proc. Natl. Acad. Sci. U.S.A.*, **69**, 2622 (1972).
- (11) L. D. Spaulding, C. C. Chang, N.-T. Yu, and R. H. Felton, *J. Am. Chem. Soc.*, **97**, 2517 (1975).
- (12) A. Warshel, *Annu. Rev. Biophys. Bioeng.*, **6**, 273 (1977).
- (13) J. P. Collman, J. L. Hoard, N. Kim, G. Lang, and C. A. Reed, *J. Am. Chem. Soc.*, **97**, 2676 (1975).
- (14) R. C. Ladner, E. J. Heidner, and M. F. Perutz, *J. Mol. Biol.*, **114**, 385 (1977).
- (15) M. Zobrist and G. N. LaMar, *J. Am. Chem. Soc.*, **100**, 1944 (1978).
- (16) M. E. Kastner, W. R. Scheidt, T. Mashiko, and C. A. Reed, *J. Am. Chem. Soc.*, **100**, 666 (1978).
- (17) T. Mashiko, M. E. Kastner, K. Spartalian, R. W. Scheidt, and C. A. Reed, *J. Am. Chem. Soc.*, **100**, 6354 (1978).
- (18) J. H. Fuhrhop and K. M. Smith in ref 9, p 835.
- (19) N. Sadasivan, H. I. Eberspraecher, W. H. Fuchsman, and W. S. Caughey, *Biochemistry*, **8**, 534 (1969).
- (20) K. D. Hapner, R. A. Bradshaw, C. R. Hartzell, and F. R. N. Gurd, *J. Biol. Chem.*, **243**, 683 (1968).
- (21) W. M. Clark, J. F. Taylor, T. H. Davies, and C. S. Vestling, *J. Biol. Chem.*, **135**, 543 (1940).
- (22) D. H. Dolphin, J. R. Sams, and T. G. Tsing, *Inorg. Chem.*, **16**, 711 (1977).
- (23) J. M. Burke, J. R. Kincaid, S. Peters, R. R. Gagne, J. P. Collman, and T. G. Spiro, *J. Am. Chem. Soc.*, **100**, 6083 (1978).
- (24) D. M. Scholler and B. M. Hoffman in "Porphyrin Chemistry", F. R. Longo, Ed., Ann Arbor Science, Ann Arbor, Mich., in press.
- (25) T. Takano, *J. Mol. Biol.*, **110**, 533 (1977).
- (26) B. D. Olafson and W. A. Goddard, *Proc. Natl. Acad. Sci. U.S.A.*, **74**, 1315 (1977).
- (27) A. Warshel, *Proc. Natl. Acad. Sci. U.S.A.*, **74**, 1789 (1977).
- (28) J. F. Kirner and W. R. Scheidt, *Inorg. Chem.*, **14**, 2081 (1975).
- (29) (a) T. Iizuka and M. Kotani, *Biochim. Biophys. Acta*, **181**, 275 (1969); **194**, 351 (1969); (b) J. G. Beeston and P. George, *Biochemistry*, **3**, 707 (1964); (c) J. O. Alben and L. Y. Fager, *ibid.*, **11**, 842 (1972).
- (30) J. F. Deatherage, R. S. Loe, and K. Moffat, *J. Mol. Biol.*, **104**, 723 (1976).
- (31) G. Rakshit and T. G. Spiro, *Biochemistry*, **13**, 5317 (1974).
- (32) A. Lanir and A. Shejter, *Biochem. Biophys. Res. Commun.*, **62**, 199 (1975).
- (33) A. S. Brill and H. E. Sandberg, *Biophys. J.*, **8**, 669 (1968).
- (34) T. Yonetani and H. Yamamoto in "Oxidases and Related Redox Systems", Vol. 1, T. E. King, H. Mason, and M. Morrison, Eds., University Park Press, Baltimore, Md., 1973, p 279.
- (35) A. S. Brill, *Comp. Biochem.*, **14**, 447 (1966).
- (36) (a) P. George and R. L. J. Lyster, *Proc. Natl. Acad. Sci. U.S.A.*, **44**, 1013 (1958); (b) P. George, R. L. J. Lyster, and J. Beeston, *J. Biol. Chem.*, **236**, 3246 (1961).
- (37) (a) G. N. La Mar, *J. Am. Chem. Soc.*, **95**, 1662 (1973); (b) R. V. Snyder and G. N. La Mar, *ibid.*, **98**, 4419 (1976).
- (38) P. D. Pulsinelli, M. F. Perutz, and R. L. Nagel, *Proc. Natl. Acad. Sci. U.S.A.*, **70**, 3870 (1973).
- (39) R. K. Gupta and G. R. Schonbaum, *Proc. Fed. Biol. Sci.*, **36**, 756 (1977).
- (40) S. Vuk-Pavlovich and Y. Siderer, *Biochem. Biophys. Res. Commun.*, **79**, 885 (1977).
- (41) T. C. Strekas and T. G. Spiro, *Biochim. Biophys. Acta*, **351**, 237 (1974).
- (42) T. Kitagawa, Y. Ozaki, Y. Kyogoku, and T. Horio, *Biochim. Biophys. Acta*, **495**, 1 (1977).
- (43) S. Taniguchi and M. D. Kamen, *Biochim. Biophys. Acta*, **74**, 438 (1963).
- (44) A. Ehrenberg and M. D. Kamen, *Biochim. Biophys. Acta*, **102**, 333 (1965).
- (45) M. M. Maltempo, T. H. Moss, and M. A. Cusanovich, *Biochim. Biophys. Acta*, **342**, 290 (1974).
- (46) J. S. Leigh, M. M. Maltempo, P. I. Ohlsson, and K. G. Paul, *FEBS Lett.*, **51**, 304 (1975).
- (47) P. V. Huong and J.-C. Pommier, *C. R. Acad. Sci., Ser. C*, **285**, 519 (1977).
- (48) J. S. Falk, "Porphyrins and Metalloporphyrins", American Elsevier, New York, 1964, p 92.
- (49) S. Sunder and H. J. Bernstein, *J. Raman Spectrosc.*, **5**, 351 (1976).
- (50) M. Abe, T. Kitagawa, and Y. Kyogoku, *Chem. Lett.*, 249 (1976).
- (51) H. Susi and J. S. Ard, *Spectrochim. Acta, Part A*, **33**, 561 (1977).
- (52) D. L. Cullen and E. F. Meyer, Jr., *J. Am. Chem. Soc.*, **96**, 2095 (1974).
- (53) E. F. Meyer, Jr., *Acta Crystallogr., Sect. B*, **28**, 2162 (1972).
- (54) (a) D. M. Collins, R. Countryman, and J. L. Hoard, *J. Am. Chem. Soc.*, **94**, 2066 (1972); (b) L. J. Radonovich, A. Bloom, and J. L. Hoard, *ibid.*, **94**, 2073 (1972).
- (55)  $P_N - P_C = (\sum_{i=1}^4 m_i(X_i - x_N)) \sin \theta / M$  where  $X_i - x_N$  are the projections along X, the pyrrole bisector, of the distance to N of the four pyrrole and one methine carbon atoms;  $m_i = 12$ , the mass of a carbon atom, and  $M = 74$ , the sum of the 5C + N atomic masses.
- (56) J. L. Hoard and W. R. Scheidt, *Proc. Natl. Acad. Sci. U.S.A.*, **71**, 1578 (1974); **70**, 3919 (1973).
- (57) E. B. Wilson, J. C. Decius, and P. C. Cross, "Molecular Vibrations", McGraw-Hill, New York, 1955.
- (58) J. C. Duinker and I. M. Mills, *Spectrochim. Acta, Part A*, **24**, 417 (1968).
- (59) (a) J. L. Hoard, *Science*, **174**, 1295 (1971); (b) D. F. Koenig, *Acta Crystallogr.*, **18**, 663 (1965).